Contents lists available at ScienceDirect

Solid State Ionics

Solid solution formation, densification and ionic conductivity of Gd- and Sm-doped ceria

S.L. Reis, E.C.C. Souza, E.N.S. Muccillo *

Instituto de Pesquisas Energéticas e Nucleares-IPEN, PO BOX 11049, S. Paulo, SP, 05422-970, Brazil

ABSTRACT

The processes of solid solution formation, densification and electrical conductivity in samaria and gadolinia-doped ceria solid electrolytes were studied by Raman spectroscopy, density and impedance spectroscopy measurements. Bulk specimens of $Ce_{0.9}Gd_{0.1}O_{1.95}$ and $Ce_{0.8}Sm_{0.2}O_{1.9}$ were prepared by solid state reactions at several dwell temperatures and holding times. Hydrostatic density results show a fast increase in sintered density up to 1 h holding time. Raman spectra of specimens sintered for 1 h show a prominent band at 463 cm^{-1} assigned to the cubic fluorite-type lattice of cerium oxide, and low-intensity bands at 344 and 363 cm^{-1} attributed to free samarium and gadolinium sesquioxides, respectively. Solid solution completion was achieved only at temperatures above 1400 °C. Electrical conductivity measurements were used to study mass transport. Analysis of impedance data allowed for determining the activation energy for cation diffusion in $Ce_{0.9}Gd_{0.1}O_{1.95}$ and $Ce_{0.8}Sm_{0.2}O_{1.9}$ sintered specimens.

© 2010 Elsevier B.V. All rights reserved.

1. Introduction

Cerium oxide can form solid solutions with rare earth oxides in a wide compositional range. The available data, first summarized in [1], show that the rare earth oxides have high solubility in cerium oxide. These solid solutions exhibit high ionic conductivity at intermediate temperatures (500–700 °C), and have been proposed as solid electrolytes in intermediate temperature solid oxide fuel cells (IT-SOFCs) [2].

One of the main disadvantages of these solid solutions is their relatively low sinterability, mainly when they are prepared by solid state reactions [3]. Mass transport is an important phenomenon in ceramic materials for the fabrication of technological devices, their properties and overall stability. The mass transport in these materials occurs by diffusion of chemical species and is responsible for solid solution formation, control of the sintering rate, solid state reactions and grain growth [4].

The diffusion process accounts for the mass transport during sintering, the grain growth, some phase transitions and the electrical conductivity. The main experimental techniques for the study of diffusion in solids are based on the radioactive tracer method, on electron microprobe analysis, on secondary ion mass spectroscopy analysis and on autoradiography methods [4].

Several phenomena are dependent on mass transport and may be monitored to obtain a diffusion coefficient. The electrical conductivity determined by impedance spectroscopy has been already used to

obtain the diffusion coefficient in some electrochemical systems including thin films, monolithic ceramics and membranes [5,6]. The sintering process of polycrystalline oxide ceramics is controlled by the slowest diffusing species. In doped zirconia, for example, the oxygen ion has high mobility and a diffusion coefficient about six orders of magnitude higher than that of zirconium. Therefore, the diffusion of zirconium cations determines the rate at which the atomic arrangement, the structural homogenization, the kinetics of sintering and grain growth, and the phase stabilization occur. Whereas the diffusion of both cation and anion species in zirconia-based solid electrolytes was throughout studied, few works may be found in doped-ceria ceramics [7,8]. Oxygen self-diffusion was studied by Kamiya [9] and Manning [8] in pure and gadolinia-doped ceria, respectively.

In this work, the solid solution formation, the densification and the sintering processes in $Ce_{0.9}Gd_{0.1}O_{1.95}$ and $Ce_{0.8}Sm_{0.2}O_{1.9}$ were studied by Raman spectroscopy, by density measurements and by the electrical conductivity determined by impedance spectroscopy, to contribute for the knowledge of the mass transport-dependent processes in these materials.

2. Experimental

Cerium oxide (CeO_2, 99.9, Aldrich), gadolinium oxide (Gd_2O_3, 99.9%, Alfa Ventron), and samarium oxide (Sm_2O_3, 99.9, BDH) were used as starting materials. Solid solutions of $Ce_{0.9}Gd_{0.1}O_{1.95}$ and $Ce_{0.8}Sm_{0.2}O_{1.9}$ were prepared by solid state reactions. The starting oxides were mechanically mixed in the stoichiometric proportions for 6 h in alcoholic medium using zirconia balls for homogenization. Cylindrical

* Corresponding author. Tel.: +55 11 31339203; fax: +55 11 31339276.
E-mail address: enavarro@usp.br (E.N.S. Muccillo).

pellets were prepared by cold pressing followed by sintering at several dwell temperatures and holding times.

Sintered density values were determined by the water immersion method. Structural characterization was carried out by Raman spectroscopy measurements (Renishaw InVia Raman Microscope) using the 633 nm exciting radiation of a He–Ne laser. The electrical conductivity was determined by impedance spectroscopy measurements using a low-frequency impedance analyzer (4192A Hewlett Packard) in the 5 Hz to 13 MHz frequency range. Silver paste was used as electrode material.

3. Results and discussion

3.1. Densification and solid solution formation

The evolution of the sintered density of $Ce_{0.8}Sm_{0.2}O_{1.9}$ with the dwell temperature is shown in Fig. 1a. An almost linear increase of the apparent density is observed up to 1550 °C. Similar observation holds for gadolinium-doped ceria solid electrolytes. For higher temperatures, loss of oxygen due to cerium reduction may produce deviation from stoichiometry, lowering the sintered density [10]. The sintering density behavior upon the holding time for $Ce_{0.9}Gd_{0.1}O_{1.95}$ is shown in Fig. 1b. A fast increase in the density occurs up to 1 h at each temperature, and for longer holding times the densification is slowed down tending to a steady state. This result indicates that densification occurs mainly in the

first hour of heat treatment independent on the dwell temperature, and that longer holding times favored the grain growth process. The same effects were obtained for samarium-doped ceria.

Solid solution formation study was carried out in samples heat treated for 1 h at 700, 800, 900, 1000, 1100, 1200, 1300, 1400 and 1500 °C. Fig. 2 shows Raman spectroscopy spectra for $Ce_{0.9}Gd_{0.1}O_{1.95}$ (Fig. 2a) and $Ce_{0.8}Sm_{0.2}O_{1.9}$ (Fig. 2b) after thermal treatment at 1100 °C/ 1 h. The full spectrum exhibits a prominent Raman band centered at
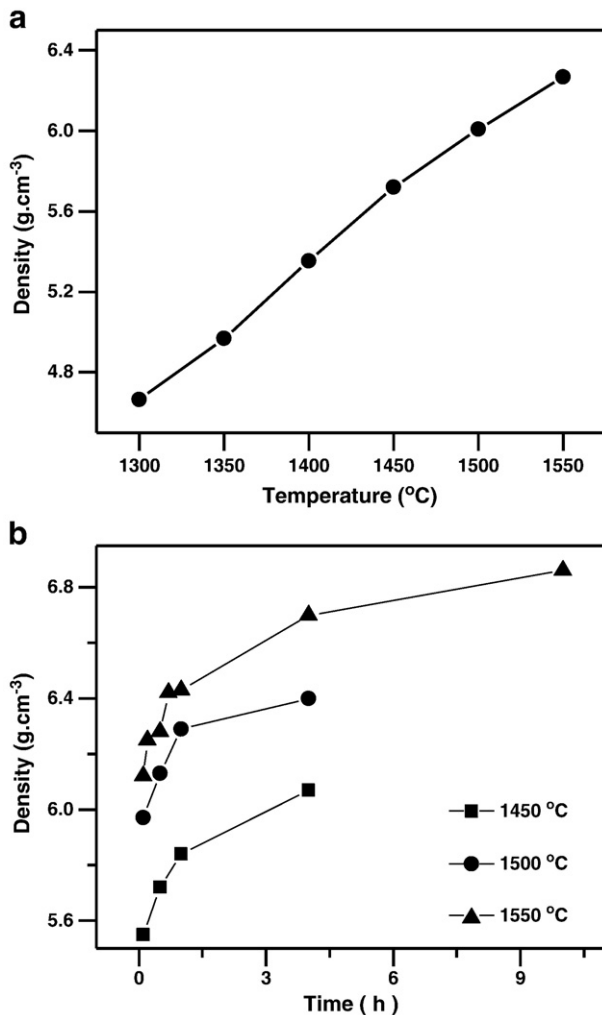

Fig. 1. Evolution of sintered density with (a) the dwell temperature ($Ce_{0.8}Sm_{0.2}O_{1.9}$), and with (b) the holding time ($Ce_{0.9}Gd_{0.1}O_{1.95}$).
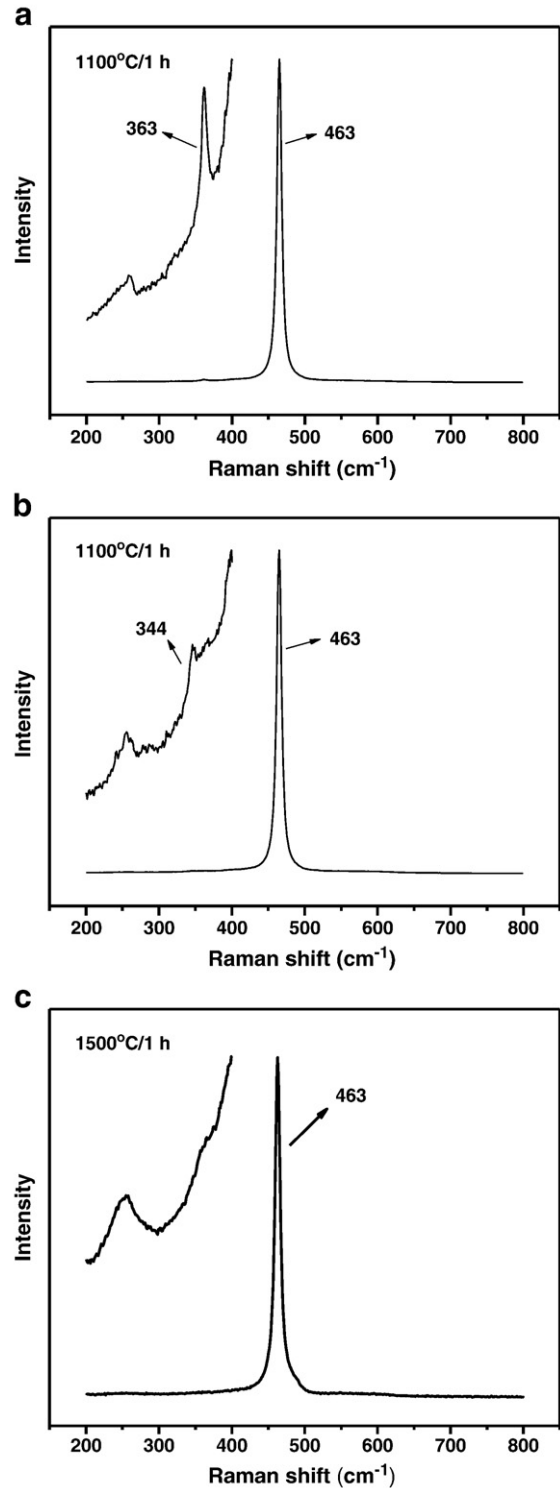
Fig. 2. Raman spectra of (a) $Ce_{0.9}Gd_{0.1}O_{1.95}$ and (b) $Ce_{0.8}Sm_{0.2}O_{1.9}$ after 1100 °C, and (c) $Ce_{0.9}Gd_{0.1}O_{1.95}$ after 1500 °C.

463 cm^{-1} characteristic of the F_{2g} triple degenerated mode of the fluorite lattice. In the left-hand side of each figure, a second spectrum, registered with longer counting time, may be observed. In these spectra, the Raman bands at 344 and 363 cm^{-1} are assigned to free Sm_2O_3 and Gd_2O_3 [11], respectively, with cubic symmetries showing that at such high temperature the solid solution was not completed yet. These Raman band characteristics of rare earth sesquioxides disappeared only after heat treatment at temperatures above 1400 °C, as shown in Fig. 2c for $Ce_{0.9}Gd_{0.1}O_{1.95}$ thermally treated at 1500 °C for 1 h. Therefore, up to that temperature, a significant amount of the energy supplied to the system is used for solid solution formation.

3.2. Ionic conductivity

Ionic conductivity measurements were carried out on specimens sintered at several dwell temperatures and holding times. As the ionic conductivity results are qualitatively similar for both solid electrolytes, for the sake of brevity, only results obtained for samarium-doped ceria will be shown.

The Arrhenius plots of Fig. 3 show that the grain conductivity (top) increases with increasing dwell temperature. The grain conductivity of $Ce_{0.8}Sm_{0.2}O_{1.9}$ sintered at 1550 °C is more than one order of magnitude higher than that of the same material sintered at 1450 °C. The grain boundary conductivity (bottom) has a similar behavior, but the difference in the grain boundary conductivity for the same specimens is less than half order of magnitude. This difference in the ionic conductivity is probably related to the porosity (Fig. 1), once solid solution is completely formed at such high temperatures.

The influence of the holding time on the ionic conductivity of $Ce_{0.8}Sm_{0.2}O_{1.9}$ sintered at 1550 °C is shown in Fig. 4. The grain (a) and the grain boundary (b) conductivities increase with the holding time up to 10 h, and decrease beyond that value. Though the increase in the holding time promotes grain growth, it seems to be beneficial to improve the ionic conductivity of these solid electrolytes. The increase of the ionic conductivity of both grain and grain boundaries with the sintering time may be related to several factors. Increased grain conductivity might be a consequence of impurity segregation to grain boundaries or due to dissolution of some impurity, which in some way contributes for improving this property, for example, by improving cation radius mismatch. Increase in the grain boundary conductivity may also be related to impurity segregation or dissolution and, in addition, it may be a consequence of changes in the interface and/or space charge layer structures. Increase in the grain boundary conductivity of 10 mol% gadolinia-doped ceria has been reported for a post-sintering heat treatment at 1350 °C, and was attributed to changes in the physico-chemical properties of grain boundaries [12]. For sintering times of about 14 h, both the grain and the grain boundary conductivities decrease. This overall decrease in the electrolyte conductivity may result from overfiring that is responsible for a number of deleterious effects occurring in ceramic materials, whenever excessive high dwell temperatures and/or sintering times are used [13].
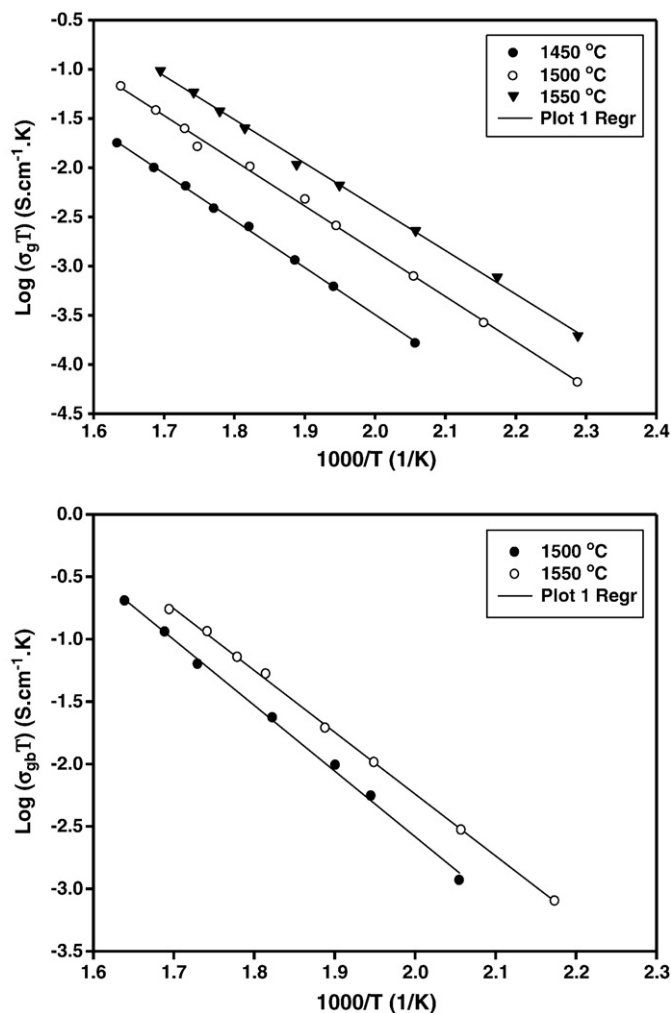

Fig. 3. Arrhenius plots of the grain (top) and grain boundary (bottom) conductivities in $Ce_{0.8}Sm_{0.2}O_{1.9}$ sintered at several temperatures for 5 h.
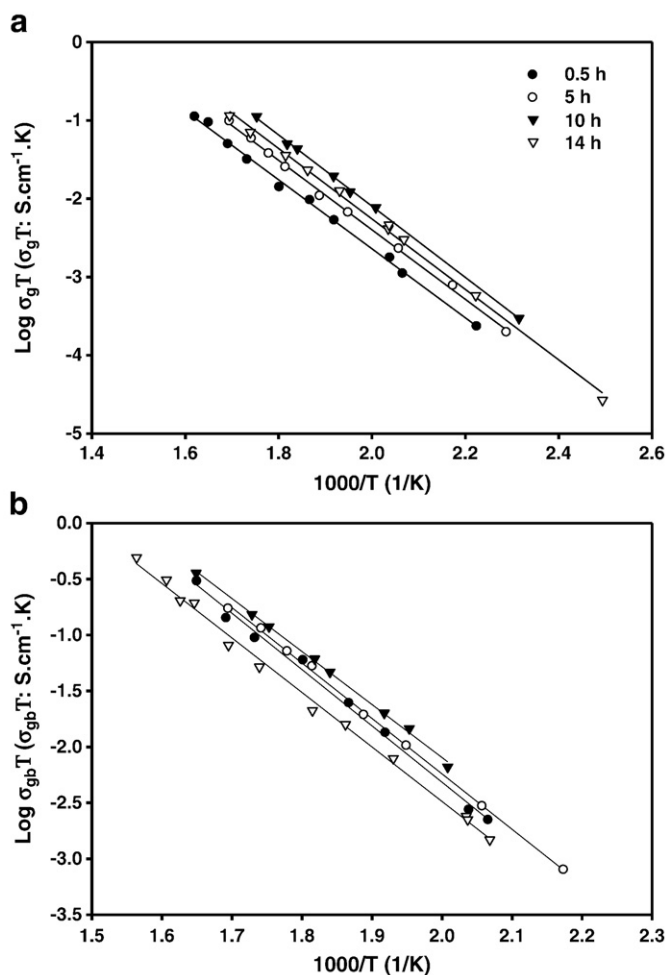

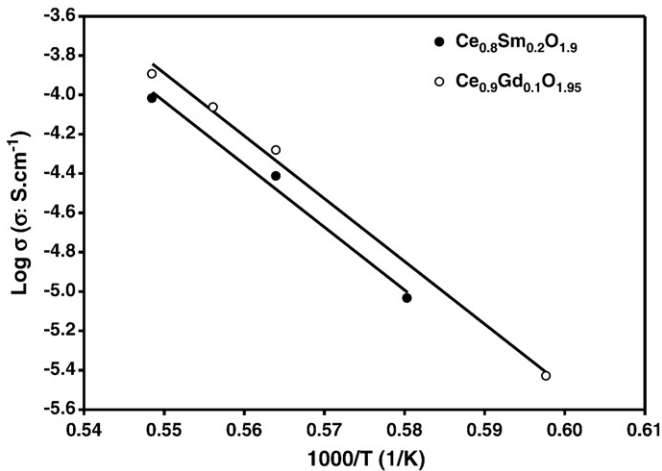Fig. 4. Arrhenius plots of the (a) grain and (b) the grain boundary conductivities in $Ce_{0.8}Sm_{0.2}O_{1.9}$ sintered at 1550 °C for several holding times.

Fig. 5. Variation of grain conductivity with reciprocal sintering temperature for $Ce_{0.8}Sm_{0.2}O_{1.9}$ and $Ce_{0.9}Gd_{0.1}O_{1.95}$.

The activation energy values decrease with increasing the dwell temperature. For $Ce_{0.9}Gd_{0.1}O_{1.95}$ they are in the 0.75–0.79 (grain) and 0.91–0.97 eV (grain boundary) ranges. For $Ce_{0.8}Sm_{0.2}O_{1.9}$ these figures are slightly higher (0.89–0.91 for grains and 0.94–1.03 eV for grain boundaries).

Fig. 5 shows the temperature dependence of the grain conductivity of $Ce_{0.9}Gd_{0.1}O_{1.95}$ and $Ce_{0.8}Sm_{0.2}O_{1.9}$ on the reciprocal of the sintering temperature. In this case, only measurements taken at temperatures above that of solid solution formation were considered. A linear behavior may be seen, as expected for a thermally activated process. The activation energy for sintering obtained from these plots is 6.33 and 6.34 eV for $Ce_{0.9}Gd_{0.1}O_{1.95}$ and $Ce_{0.8}Sm_{0.2}O_{1.9}$, respectively. These figures are higher than that of yttria-stabilized zirconia (~4.5 eV) explaining the relatively low sinterability of ceria-based solid solutions compared to stabilized zirconias.

4. Conclusions

The solid solution formation process of Sm and Gd ions in cerium oxide was successfully evaluated by Raman spectroscopy and electrical conductivity measurements. The obtained results show that high sintering temperatures and large holding times are necessary for complete solid solution formation. The activation energy value for sintering, determined by electrical conductivity measurements, for these solid solutions is about 6.33 eV.

Acknowledgement

References

[1] T.H. Etsell, S.N. Flengas, Chem. Rev. 70 (1970) 339.
[2] H. Inaba, H. Tagawa, Solid State Ionics 83 (1996) 1.
[3] J. van Herle, T. Horita, T. Kawada, N. Sakai, H. Yokokawa, M. Dokiya, J. Am. Ceram. Soc. 80 (1997) 933.
[4] A. Atkinson, in: R.W. Cahn, P. Haasen, E.J. Kramer (Eds.), Materials Science and Technology, a Comprehensive Treatment, Structure and Properties of Ceramics, 11, VCH, Weinheim, Germany, 1994, p. 295.
[5] J.R. Macdonald, Impedance Spectroscopy-Emphasizing Solid Materials and Systems, Wiley Interscience, New York, 1987, p. 29.
[6] F.C. Fonseca, E.N.S. Muccillo, R. Muccillo, Solid State Ionics 149 (2002) 309.
[7] M. Kamiya, E. Shimada, Y. Ikuma, J. Ceram. Soc. Jpn. 106 (1998) 1023.
[8] P.S. Manning, J.D. Sirman, J.A. Kilner, Solid State Ionics 93 (1997) 125.
[9] M. Kamiya, E. Shimada, Y. Ikuma, M. Komatsu, H. Haneda, J. Electrochem. Soc. 147 (2000) 1222.
[10] E.C.C. Souza, E.N.S. Muccillo, J. Alloy Comp. 472 (2009) 560.
[11] N. Dilamar, D. Varandani, S. Mehrota, H.K. Poswal, S.M. Sharma, A.K. Bandyopadhyay, Nanotechnology 19 (2008) 115703.
[12] D.-S. Kim, P.-S. Cho, J.-H. Lee, D.-Y. Kim, S.B. Lee, Solid State Ionics 177 (2006) 2125.
[13] D.W. Kingery, H.K. Bowen, D.R. Uhlmann, Introduction to Ceramics, John Wiley & Sons, New York, 1975, p. 507.